

An above-room-temperature switchable molecular dielectric with a large dielectric change between high and low dielectric states

DU Yang, HAO HuiMin, ZHANG QianChong, ZHAO HaiXia^{*}, LONG LaSheng^{*},
HUANG RongBin & ZHENG LanSun

State Key Laboratory for Physical Chemistry of Solid Surfaces, Department of Chemistry, College of Chemistry and Chemical Engineering,
Xiamen University, Xiamen 361005, China

Received November 8, 2012; accepted November 28, 2012; published online February 22, 2013

Dielectric anisotropy of anilinium perchlorate is investigated at various temperatures. Crystal structures at different temperatures reveal that significant dielectric change between low and high dielectric states is closely related to the disorder of the anilinium cation and perchlorate anion at high dielectric state; meanwhile, the conductivity after phase transition also contributes a lot to the high dielectric state.

switchable molecular dielectric, ionic conductivity, dielectric anisotropy, phase transition

1 Introduction

Switchable molecular dielectrics, which undergo transitions between high and low dielectric states, are promising materials potentially applicable in data communication and signal processing [1–3]. In principle, switchable molecular dielectrics could arise from the reorientation of the polar guests in metal-organic frameworks [4, 5], or order-disorder molecular-ionic solid, such as pyridinium salts [6]. Some switchable molecular dielectrics have been successfully prepared on the basis of these principles. On the one hand, synthesis of such kind of switchable molecular dielectrics remains a great challenge due to the difficulty in keeping the dielectric constant almost unchanged respectively at high and low dielectric states. On the other hand, the switchable molecular dielectrics synthesized so far either suffer from lower phase transition temperature, or relatively small dielectric change between high and low dielectric states. As a result, practical applications of those materials are in fact limited.

Anilinium perchlorate, similar to those of pyridinium salts, is a molecular-ionic solid. Previous study showed that a first order phase transition occurred at about 220 K [7]. A possible mechanism of the phase transition was suggested in relation to disorder of the hydrogen atoms on nitrogen atoms [7]. Owing to the existence of a perchlorate anion in this compound, it is expected to exhibit an above-room temperature phase transition connected with the ordering of the perchlorate anion [3, 8, 9]. On the other hand, the relatively high temperature phase transition would in turn increase the dielectric constant of the compound due to the high temperature favoring the disorder of ClO_4^- . Here we report dielectric anisotropy of a molecular-ionic anilinium perchlorate, namely $\text{C}_6\text{H}_8\text{NClO}_4$ (APC for short), in the temperature range from 300 to 460 K. Surprisingly, the phase transition temperature of APC is up to 442 K, while its dielectric change between low and high dielectric states is up to 137 along the *a* axis.

2 Experimental

2.1 General experimental section

Chemicals were used as purchased from commercial ven-

^{*}Corresponding authors (email: lslong@xmu.edu.cn; hxzhao@xmu.edu.cn)

dors without further purification. The C, H, and N microanalyses were carried out with a Vario EL III elemental analyzer.

2.2 Synthesis of APC

Compound APC was synthesized by the reaction of perchloric acid and aniline in water as described in the previous literature [7]. Perchloric acid (4 mmol, 2 mol L⁻¹) and aniline (4 mmol, 0.366 mL) were dissolved into 10 mL deionized water, while stirring at room temperature. The mixture solution was kept at room temperature in dark place. Colourless sheet crystals were obtained in about 55% yield (based on aniline) after about one month. IR (KBr, cm⁻¹): 3444.1 (m), 2907.8 (s), 2589.3 (m), 1599.4 (w), 1562.3 (m), 1515.4 (w), 1493.7 (s), 1193.7 (w), 1144.8 (s), 1113.6 (s), 1089.3 (s), 1030.3 (w), 743.9 (s), 682.6 (m), 627.4 (s), 525.5 (w), 475.5 (w); Anal. Calcd for **1**: C: 37.23, N: 7.24%, H: 4.16%. Found: C: 37.27%, N: 7.26%, H: 4.11%.

2.3 X-Ray crystal data collection and analysis

Single-crystal X-ray structure determination: Data collections were performed on an Oxford Gemini S Ultra CCD area detector using Mo-K α radiation at 298 K, 453 K for APC with the same single-crystal. Absorption corrections were applied by using the multi-scan program. The structures were solved by direct methods, and non-hydrogen atoms were refined anisotropically by least-squares on F^2 using the SHELXTL-97 program [10]. All the hydrogen atoms were generated geometrically.

2.4 DSC and TG measurements

DSC (differential scanning calorimetry) measurements were performed on the NETZSCH DSC 200F3 with sweeping rate of 10 K/min under nitrogen atmosphere. The TG curve was measured on Thermal Analyzer SDT Q600 with sweeping rate of 10 K/min under air atmosphere.

2.5 The impedance and dielectric measurements

Temperature-dependent a.c. impedance plots and dielectric constants were performed on Wayne Kerr 6500B by using two-probe a.c. impedance method in frequency range from 1 kHz to 10 MHz. The single crystals were placed into American Sigma chamber in order to realize variation of the temperature. The electric contacts were prepared with silver paste to attach 25- μ m gold wires to the single crystal.

3 Results and discussion

3.1 Thermal analysis and dielectric properties

TG analysis clearly demonstrated that APC is stable up to

500 K. As shown in Figure 1(a), and endothermic peak at 442 K in the heating process and an exothermic peak at 418 K in the cooling process were observed. The DSC result indicates that the phase transition is reversible. The XRD patterns were performed at 298 K and 453 K, which are corresponding to that before and after phase transition temperatures. All the patterns fit very well with the curves simulated based on X-Ray single crystal data. The XRD patterns at 453 K change a lot comparing to that at 298 K. Meanwhile, after cooling to 298 K, the XRD patterns fit very well with the patterns at 298 K (before phase transition). It further demonstrated that APC undergoes reversible phase transition (Figure 2). Based on the DSC data, the ΔH and $\Delta S (= \Delta H/T_c)$ are estimated to be 3.4 kJ mol⁻¹ and 7.65 J mol⁻¹K⁻¹ respectively. According to $\Delta S = R \ln(N_2/N_1)$,

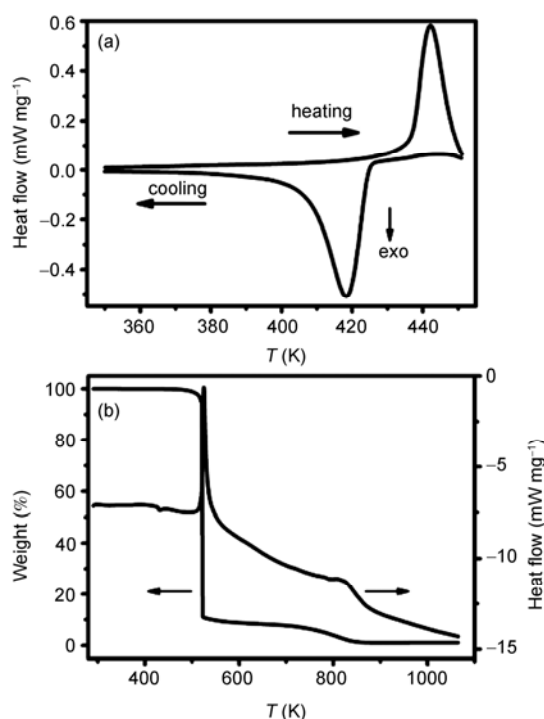


Figure 1 DSC curves (a) and TG curves (b) of APC.

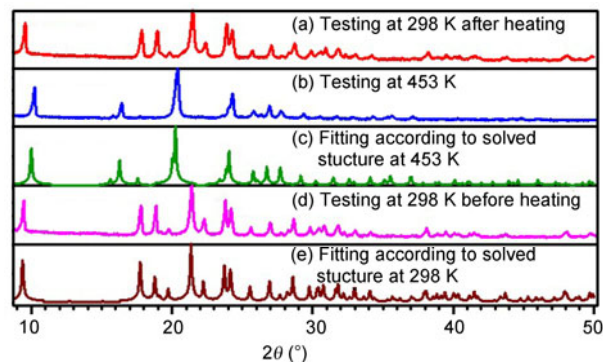


Figure 2 The XRD patterns at different temperatures exhibiting reversible phase transition.

where R , N_1 and N_2 are the gas constant and the numbers of possible orientations of low and high temperature phases, N_2/N_1 is about 5/2, indicating that the phase transition is of typical order-disorder type [11].

Figure 3 showed the dielectric constants of APC along a , b and c axes in the temperature range from 300 to 460 K. At $f = 10$ kHz, the dielectric constant of APC along a axis almost keeps a constant (cal. 14) from 300 to 434 K, then it abruptly increases to 137 at phase transition temperature and keeps a constant after phase transition. The dielectric change before phase transition (low dielectric state) and after phase transition (high dielectric state) in APC is significantly larger than that in $(\text{Him})_2[\text{KFe}(\text{CN})_6]$, $[\text{Mn}_3(\text{HCOO})_6](\text{H}_2\text{O})(\text{CH}_3\text{OH})$ and the similar compound 4-methylanilinium perchlorate previously reported [3–5]. Its phase transition temperature is also significantly higher. Similarly, the dielectric constant of APC along the b axis also exhibits temperature-dependent behavior. However, its dielectric constant significantly decreases with the increase of temperature after phase transition. In contrast, only a small dielectric anomaly is observed along the c axis in the whole temperature range. These results indicate that dielectric constants of APC are crystal-axis dependent. Consistently, in the cooling process the dielectric constants along a , b and c axes also exhibit crystal-axis dependent behavior (Figure S3–S4). However, the dielectric peaks along a and b axes appeared at 415 and 453 K respectively at $f = 10$ kHz (Figure S3), significantly different from those in the heating process. In contrast, the dielectric peak along c axis in the cooling process appeared at 441 K at $f = 10$ kHz (Figure S3),

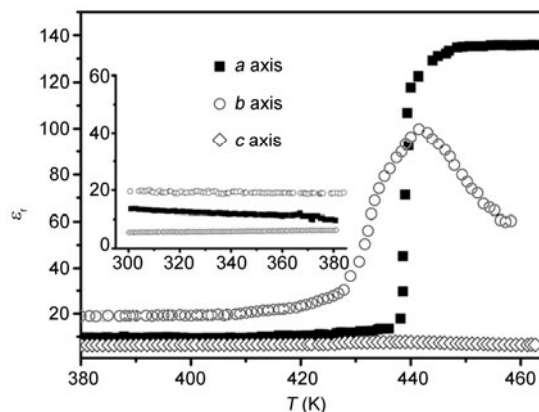


Figure 3 The dielectric constant of APC measured as a function of temperatures along the different axes at 10 kHz.

comparable to that in the heating process. The thermal dielectric hysteresis is coincident with the DSC, which shows that it may be related to the dynamics process in this system.

Figure 4 shows dielectric imaginary parts (ϵ'') at different temperatures along a , b and c axes respectively. The dielectric imaginary parts (ϵ'') exhibits the similar temperature- and frequency-dependent behavior as that of the dielectric constant, and dielectric imaginary part (ϵ'') along a axis is significantly larger than that along b axis, while the later is significantly larger than that along c axis. Based on the dielectric imaginary parts (ϵ'') and its frequency-dependent behavior, it is concluded that the contribution of long-range displacement of mobile charge carriers is ineligible [12].

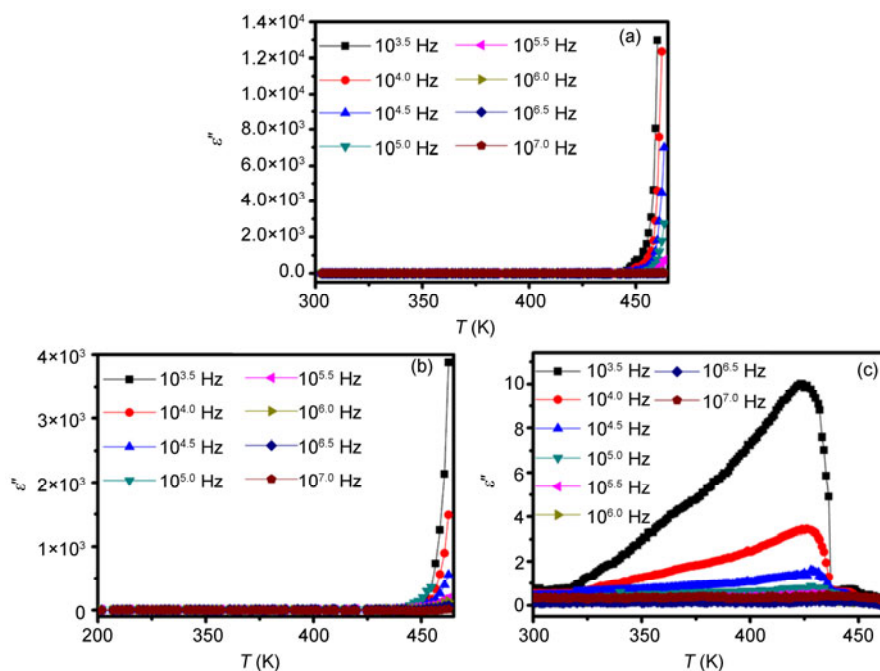


Figure 4 The imaginary parts of the dielectric (ϵ'') along a , b and c axes.

3.2 Crystal structures

Although the room temperature crystal structure of APC is already known, we studied it here to discuss the dielectric and impedance properties. The crystal structure at 298 K [7, 13] revealed that it crystallized in non-centrosymmetric space group $P2_12_12_1$ (No. 19) with one anilinium cation and one perchlorate anion in an asymmetric unit [7]. Each perchlorate anion is hydrogen-bonded to three adjacent anilinium cations respectively through its three O atoms as proton acceptors to form a 1D chain structure. Adjacent 1D chain structures are hydrogen-bonded into a 2D structure through the fourth O atom of perchlorate anion from one 1D chain as a proton acceptor and anilinium cation from adjacent chains as a proton donor. Extension of the 2D structure through van der Waals Force generates a 3D supramolecular architecture as shown in Figure 5.

To reveal the unique crystal-axis dependence of dielectric constant in APC, crystal structure of APC at 453 K (namely APC(a)) was measured. As shown in Figure 6, although the asymmetric unit in APC(a) also consists of one anilinium cation and one perchlorate anion, owing to the phenyl group in the anilinium cation alternately locating three positions, and the perchlorate anion disordered over two positions, APC(a) crystallizes in a centrosymmetric space group $Pmmn$ (No. 59). Each perchlorate anion is hydrogen-bonded to two adjacent anilinium cations respectively through its O atoms as proton acceptors to furnish a 1D chain structure (Figure 6(b)). Connections of adjacent 1D chains through hydrogen-bonding interactions between the perchlorate anion and anilinium cation generate a 2D structure (Figure 6(c)), which is further extended into a 3D supramolecular architecture of APC(a) through van der Waals Force (Figure 6(d)). Although the quality of the solved crystal structure at 453 K is rather poor, the experiment XRD patterns of APC at 453 K matched very well with the fitting data simulated based on the solved structure

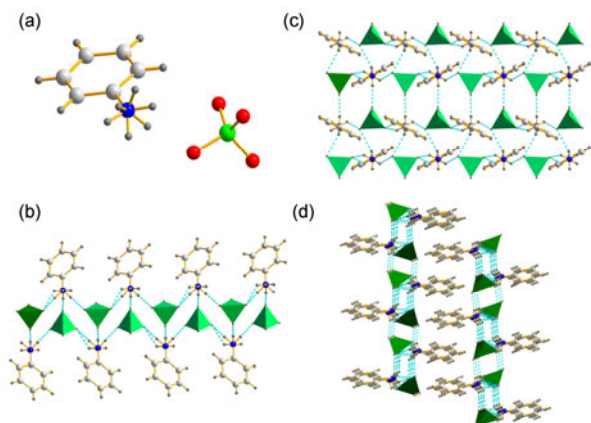


Figure 5 (a) The asymmetric unit in APC; (b) the 1D chain structure in APC viewed along $[0,1,1]$ direction; (c) the 2D structure in APC viewed along the c axis; (d) the 3D chain structure of APC along the a axis.

at 453 K (Figure 2), which shows that the solved 453 K structure is believable.

However, a , b , and c axes at 298 K is corresponded to a , b and c axes at 453 K separately. The c axis is halved at 453 K comparing to that at 298 K. The diffraction spots at 453 K decrease obviously although the exposure time was longer than that at 298 K, which proved that the lattice doubly reduced at high temperature (Figure 7) [11].

The low-high dielectric switchable behavior and axes-dependent anisotropy are mostly caused by two factors below: (1) Basing on the dielectric loss and its frequency-dependent behavior, the ionic (or protonic) conductivity contributes a lot to the high dielectric after phase transition; (2) the large change of dipole movement (the reorientation motion of the ClO_4^- anion and anilinium cation along different axes) within and between layers before and after phase transition.

In order to prove the different mobility of proton existing in this system at different temperatures, the impedance of APC at room temperature (300 K) to 460 K was investigated. Figure 8 shows that the impedance plots of APC exhibit obvious semi-circle from 446 to 463 K along a axis, which confirmed that APC at high temperature stage exhibits the dominant of large conductivity (about 9.3×10^{-6} S/cm at 463

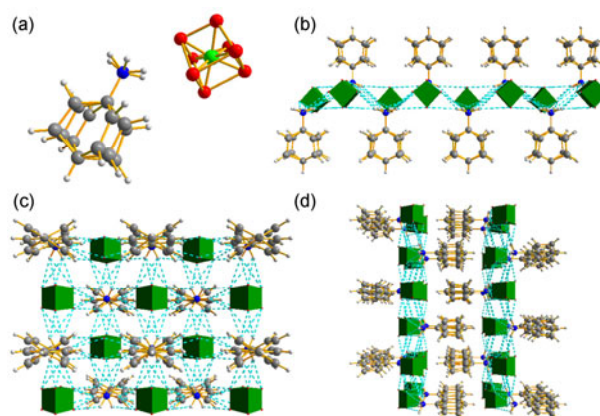


Figure 6 (a) One molecular of APC(a); (b) the 1D chain structure in APC(a) viewed along the b axes; (c) the 2D structure in APC(a) viewed along the c axes; (d) the 3D structure of APC(a) viewed along the a axis.

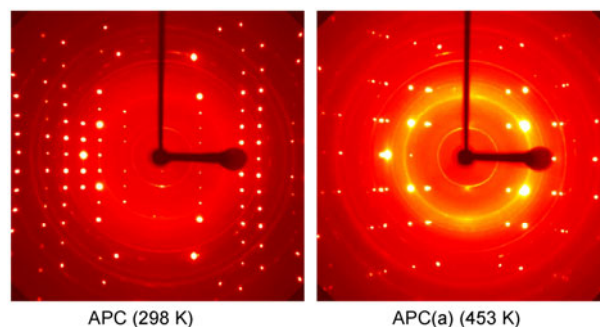


Figure 7 The diffraction patterns along c directions for APC at 298 K and 453 K.

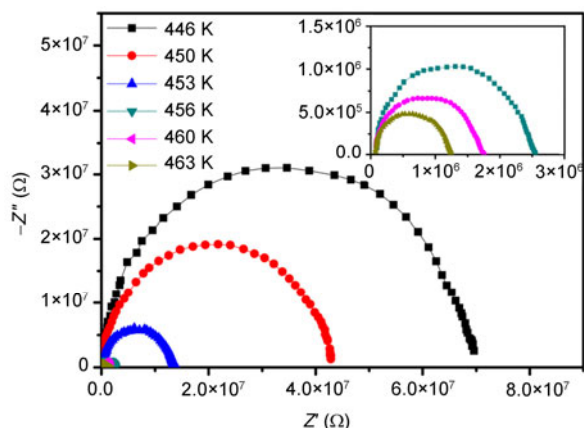


Figure 8 The impedance of APC at different temperatures along a axis.

K). Figure S6 shows that the impedance of APC exhibits a depressed arc at low temperature stage along a axis, it is evident that the conductivity is not predominated. The conductivity along b axis exhibits the similar behavior as that of a axis (Figure S6), meanwhile, the only difference is that the conductivity is slightly lower (about 5.4×10^{-6} S/cm at 463 K). The conductivity along c axis is the lowest (about 5.7×10^{-9} S/cm at 463 K), and only up to 463 K, the impedance exhibits a uncompleted semi-circle. It is noticeable that the defects created during the strong phase transition with large change of volume may result in additional conductivity.

After phase transition, the ionic conductivity indeed contributed a lot to the high dielectric state. However, the conductivity along a , b and c axes (Figure 8, Figure S7, S8) all increases with the increasing temperature at high temperature phase, the dielectric constant keeps almost a constant along a axis, and significantly decreases with the increase of temperature after phase transition along b axis. It is contrary to the trend of the conductivity-temperature. So, we concluded that there should be some other factors resulting to the high-dielectric state. Hence, we considered the large change of dipole movement (the reorientation motion of the ClO_4^- anion and anilinium cation along different axes) within and between layers before and after phase transition. However, the difference of structure at high and low temperature phase has already confirmed that reorientation motion of the ClO_4^- anion and anilinium cation along different axes indeed occurs at high temperature phase. Before phase transition, owing to less disorder of the anilinium cation and perchlorate anion, the dielectric constant of APC is less influenced by the temperature. After the phase transition, both anilinium cation and perchlorate anion and significantly disordered, especially in the (1 1 0) plane, they exhibit the similar structural characters along a and b axes. The thermal dielectric hysteresis between the heating and cooling processes along different axes further proved that the reorientation motion of the ClO_4^- anion and anilinium cation con-

tribute to the high-low temperature switchable behavior.

4 Conclusion

In summary, we have reported dielectric anisotropy of a molecular-ionic anilinium perchlorate in the temperature range from 300 to 460 K with a single-crystal. Investigation on the temperature-dependent dielectric behavior of APC showed that its phase transition temperature is up to 442 K, while its dielectric change between low and high dielectric state is up to 137 along the a axis. Study on the crystal structures of APC at different temperatures revealed that significant dielectric change between low and high dielectric states is closely related to the disorder of the anilinium cation and perchlorate anion at high dielectric state. Unambiguously, low-high dielectric switchable behavior and axes-dependent anisotropy is the creation of the combining powers: the ionic (or protonic) conductivity and the reorientation motion of the ClO_4^- anion and anilinium cation along different axes.

This work was supported by the National Natural Science Foundation of China (21001089, 20825103, 90922031 and 21021061), the 973 project from MSTC (2012CB821704).

- Pajzderska A, Gonzalez MA, Wasicki J. Quasielastic neutron scattering study of pyridinium cation reorientation in thiourea pyridinium nitrate inclusion compound. *J Chem Phys*, 2008, 128(8): 084507(1-9); Pajzderska A, Fojud Z, Goc R, Wasicki J. Cation dynamics in pyridinium nitrate and bis-thiourea pyridinium nitrate inclusion compound studied by ^2H NMR spectroscopy. *J Phys: Condens Matter*, 2007, 19: 156220(1-12)
- Pajzderska A, Czarnecki P, Embs JP, Gonzalez MA, Journay F, Krawczyk J, Peplińska B, Wasicki J. A study of out-of-plane cation dynamics in a bis-thiourea pyridinium chloride inclusion compound. *J Phys Chem Chem Phys*, 2011, 13: 8908-8914; Pajzderska A, Gonzalez MA, Embs JP, Wasicki J. Complex dynamics of pyridinium cation in ferroelectric bis(thiourea)pyridinium iodide studied by Quasi-Elastic neutron scattering. *J Phys Chem C*, 2011, 115(31): 15164-15171
- Zhang W, Xu RJ. Distinct phase transitions and dielectric anomalies in two 4-methylanilinium salts. *Sci China Chem*, 2012, 55(2): 201-207
- Zhang W, Cai Y, Xiong RG, Yoshikawa H, Awaga K. Exceptional dielectric phase transitions in a perovskite-type cage compound. *Angew Chem Int Ed*, 2010, 49(37): 6608-6610
- Cui HB, Takahashi K, Okano Y, Kobayashi H, Wang ZM, Kobayashi A. Dielectric properties of porous molecular crystals that contain polar molecules. *Angew Chem Int Ed Engl*, 2005, 44(40): 6508-6512
- Pajak Z, Czarnecki P, Wasicki J, Nawrocik W. Ferroelectric properties of pyridinium periodate. *J Chem Phys*, 1998, 109(15): 6420-6423; Maluszyńska H, Czarnecki P, Lewicki S, Wasicki J, Gdaniec M. Structure and dynamics of ferroelectric pyridinium periodate. *J Phys: Condens Matter*, 2001, 13: 11053-1065
- Marchewka MK, Debrus S, Drozd M, Baran J, Barnes AJ, Xue D, Ratajczak H. Vibrational spectra, phase transition and nonlinear optical properties of anilinium perchlorate molecular-ionic solid. *Polish J Chem*, 2003, 77: 1625-1636

- 8 Pajak Z, Czarnecki P, Szafrńska B, Maluszyńska H, Fojud Z. Ferroelectric ordering in imidazolium perchlorate. *J Chem Phys*, 2006, 124(14): 144502(1–6)
- 9 Cai HL, Zhang W, Ge JZ, Zhang Y, Awaga K, Nakamura T, Xiong RG. 4-(cyanomethyl)anilinium perchlorate: a new displacive-type molecular ferroelectric. *Phys Rev Lett*, 2011, 107(14): 147601(1–5); Zhang Y, Awaga K, Yoshikawa H, Xiong RG. Ferroelastic phase transition and dielectric anomalies in 2,4,6-trimethylanilinium perchlorate. *J Mater Chem*, 2012, 22: 9841–9845
- 10 *SHELXTL 6.10*, Bruker Analytical Instrumentation, Madison, WI, 2000
- 11 Jain P, Ramachandran V, Clark RJ, Zhou HD, Toby BH, Dalal NS, Kroto HW, Cheetham AK. Multiferroic behavior associated with an order-disorder hydrogen bonding transition in metal-organic frameworks (MOFs) with the perovskite ABX_3 architecture. *J Am Chem Soc*, 2009, 131(38): 13625–13627; Xu GC, Ma XM, Zhang L, Wang ZM, Gao S. Order-disorder ferroelectric transition in the metal formate framework of $[NH_4][Zn(HCOO)_3]$. *J Am Chem Soc*, 2010, 132(28): 9588–9590
- 12 Ennaceur N, Jarraya K, Singh A, Ledoux-Rak I, Mhiri T. Phase transitions, ferroelectric behavior and second-order nonlinear optics of a new mixed sodium dihydrogen phosphate-arsenate. *J Phys Chem Solids*, 2012, 73(3): 418–422
- 13 Paixao JA, Matos Beja A, Ramos Silva M, Alte da Veiga L, Martin-Gil J. Crystal structure of anilinium perchlorate, $C_6H_5NH_3^+ClO_4^-$. *Z Kristallog -New Cryst Struct*, 1999, 214: 85–86